

Laboratory studies of gas phase sodium diffusion

Joel W. Ager III and Carleton J. Howard

Citation: *The Journal of Chemical Physics* **85**, 3469 (1986); doi: 10.1063/1.450970

View online: <http://dx.doi.org/10.1063/1.450970>

View Table of Contents: <http://scitation.aip.org/content/aip/journal/jcp/85/6?ver=pdfcov>

Published by the AIP Publishing

Articles you may be interested in

[Dielectric and Impedance Spectroscopic Studies on Diffuse Phase Transitions in Bismuth Sodium Titanate](#)
AIP Conf. Proc. **1372**, 154 (2011); 10.1063/1.3644436

[First laboratory observation of niobium monosulphide in the gas phase](#)
J. Chem. Phys. **92**, 7003 (1990); 10.1063/1.458240

[Absolute photodissociation cross sections of gas phase sodium chloride at room temperature](#)
J. Chem. Phys. **84**, 4378 (1986); 10.1063/1.450060

[Laboratory studies of diffuse waves in plates](#)
J. Acoust. Soc. Am. **79**, 919 (1986); 10.1121/1.393687

[Sodium Diffusion in Sodium Tungsten Bronze](#)
J. Chem. Phys. **22**, 266 (1954); 10.1063/1.1740049



Laboratory studies of gas phase sodium diffusion

Joel W. Ager III and Carleton J. Howard^{a)}

*Aeronomy Laboratory, National Oceanic and Atmospheric Administration, Boulder, Colorado 80303 and
Department of Chemistry and Biochemistry of the University of Colorado, and Cooperative Institute for
Research in Environmental Sciences, Boulder, Colorado 80303*

(Received 7 May 1986; accepted 30 May 1986)

The gas phase diffusion coefficients of Na in Ne, N₂, and CO₂ were measured in a flow tube with an oven source and resonant fluorescence detection of Na. $D_{\text{Na,Ne}} = 209 \pm 21 \text{ cm}^2 \text{ Torr s}^{-1}$ at 281 K, $D_{\text{Na,N}_2} = 129 \pm 13 \text{ cm}^2 \text{ Torr s}^{-1}$ at 281 K, and $D_{\text{Na,CO}_2} = 134 \pm 13 \text{ cm}^2 \text{ Torr s}^{-1}$ at 281 K. $D_{\text{Na,He}}$ was measured over the temperature range 211–424 K. $D_{\text{Na,He}}(T) = (385 \pm 40)(T/300)^{(1.72 \pm 0.18)} \text{ cm}^2 \text{ Torr s}^{-1}$. The experimental results are compared with previous studies. The sticking coefficient for Na on the walls of the flow tube was determined to be approximately equal to 1 by an analysis of the diffusion coefficient data. The results for $D_{\text{Na,He}}$, $D_{\text{Na,Ne}}$, and $D_{\text{Na,Ar}}$ are compared with the predictions of Chapman–Enskog calculations using Na–noble gas potentials from recent spectroscopic measurements.

I. INTRODUCTION

The diffusion of gaseous sodium is important in combustion, low pressure lamps, and sodium cooled nuclear reactors. In addition, diffusion coefficients must be known for an accurate analysis of flow tube kinetic data,^{1,2} particularly when the sticking coefficient is approximately unity. A wide variety of experimental methods has been used to measure gas phase diffusion coefficients of sodium. In 1932, Polanyi and co-workers³ measured $D_{\text{Na,H}_2}$, $D_{\text{Na,He}}$, $D_{\text{Na,Ar}}$, $D_{\text{Na,N}_2}$, and $D_{\text{Na,pentane}}$ in a sodium diffusion flame at ~ 650 K. Spin relaxation of optically oriented Na vapor was used to measure $D_{\text{Na,H}_2}$, $D_{\text{Na,He}}$, $D_{\text{Na,Ne}}$, and $D_{\text{Na,N}_2}$ by Ramsey and Anderson⁴ in 1964 and $D_{\text{Na,He}}$ and $D_{\text{Na,Ne}}$ by Bichi *et al.*⁵ in 1980. More recently, Fairbank *et al.*⁶ measured $D_{\text{Na,He}}$, $D_{\text{Na,Ar}}$, and $D_{\text{Na,Ne}}$ by optically monitoring the transit of single Na atoms across a 590 nm wavelength laser beam. Cornelisson⁷ studied $D_{\text{Na,Ne}}$ at 530 K by observing the decay rate of the fundamental Na diffusion mode in the afterglow of a discharge in a static cell. Husain and co-workers^{8,9} reported $D_{\text{Na,He}}$, $D_{\text{Na,N}_2}$, and $D_{\text{Na,CO}_2}$ from studies near 750 K in a flash photolysis system. Silver² measured $D_{\text{Na,He}}$, $D_{\text{Na,Ar}}$, and $D_{\text{Na,N}_2}$ in a flow system very similar to the one used in the present study. In a particularly novel experiment, Coolen and Hagedoorn¹⁰ determined $D_{\text{Na,Ne}}$ at room temperature by bombarding ²⁰Ne with 20 meV protons and measuring the decay of the resultant ²⁰Na by laser induced fluorescence (LIF). In spite of the abundance of diffusion coefficient studies, when the experimental values are extrapolated to 300 K, the agreement is only fair. There is only one measurement⁸ of $D_{\text{Na,CO}_2}$ and the values reported at 724 and 824 K differ by a factor of 3. Furthermore, most studies were done at a single pressure and no study covered a pressure range of more than a factor of 10.

Our previous flow tube work¹ on the gas phase diffusion of Na in He and Ar has been extended to include the room temperature diffusion coefficients of Na in Ne, N₂, and CO₂, and the temperature dependence of $D_{\text{Na,He}}$. This study was

undertaken to provide further measurements and to test the performance of the experimental apparatus. Since Na sticks to the wall of the flow tube with approximately unit efficiency, the observed wall loss rate constant can be related to the diffusion coefficient. By measuring the wall loss rate constant over a pressure range of a factor of 30, we can detect possible systematic errors and critically examine the assumption that the sticking coefficient on the walls of the reactor is nearly equal to 1.

II. EXPERIMENTAL

The apparatus has been described in detail previously.¹ Sodium metal is heated to ~ 400 K in an oven located outside the flow tube. The Na vapor is carried through a heated inlet (~ 480 K) and into a 2.54 cm radius copper flow tube by a small flow of flush gas ($< 3 \text{ STP cm}^3 \text{ s}^{-1}$, STP = 760 Torr, 273 K). The flush gas flow is always less than 5% of the main flow. Ne and N₂ are used as both carrier and flush gases. Since it is possible that CO₂ could form low vapor pressure compounds in the hot oven, He is used as the flush gas in the measurement of $D_{\text{Na,CO}_2}$. Na is detected by resonant fluorescence at 590 nm with a detection limit of $\sim 10^4$ atom cm^{-3} using a simple discharge lamp source.

The entire oven and inlet assembly is movable. A measurement of the wall loss rate constant is made by observing the Na resonant fluorescence signal, I_{Na} , as a function of z , where z is the distance from the tip of the Na inlet to the detection region. The rate constant is calculated from the slope of a plot of $\ln I_{\text{Na}}$ vs z ,

$$k_{\text{obs}} = \frac{-v \partial(\ln I_{\text{Na}})}{\partial z}, \quad (1)$$

where k_{obs} is the first-order wall loss rate constant and v is the average flow velocity. The diffusion coefficient is obtained from k_{obs} by the method described in Sec. III.

The flow tube is wrapped with approximately 75 turns of 1/4 in. o.d. copper tubing. The tubing is connected to an insulated reservoir and circulating pump. Silicon oil heated by resistance heaters is circulated through the coils to heat the flow tube above room temperature. Ethanol cooled by

^{a)} Author to whom correspondence should be addressed at NOAA R/E/AL2, 325 Broadway, Boulder, CO 80303.

liquid N₂ flowing through a copper heat exchanger immersed in the reservoir is used to cool the flow tube. For experiments above room temperature, the temperature is controlled by setting the voltage applied to the heaters with a variac. For experiments below room temperature, the flow of vapor from the liquid N₂ is regulated with a needle valve. The flow tube temperature is measured by a thermocouple soldered to the outside of the flow tube in the approximate center of the measurement region. This temperature is stable to ± 1 K over the course of an experiment. The flow tube temperature can be varied over the range 210–430 K.

Since the diffusion coefficient depends strongly on T , it is important that the temperature be constant in the region of wall loss measurement. This was checked over the temperature range of the $D_{\text{Na,He}}$ experiments. A thermocouple probe was constructed from 0.2 mm diameter chromel and alumel wires. The wires were placed inside a 6 mm o.d. glass tube with the junction protruding 5 cm from the tip. The junction end of the glass tube was sealed with vacuum cement. The temperature probe was inserted into the flow tube through the O ring seal used for reactant gases. For typical experimental conditions, i.e., oven and inlet heated and with the carrier and flush gases flowing, the temperatures measured by the probe and by the flow tube thermocouple differed by less than 1.5 K from 7 cm upstream of the detection region and to within 10 cm of the end of the Na inlet. In order to measure the diffusion coefficient in a temperature regulated region the measurements were done with $z \geq 20$ cm, usually over the range $z = 20$ –55 cm. Due to the lower thermal conductivity of Ar, a region of uniform gas temperature could not be maintained over the length of the flow tube with Ar as the carrier gas, so no T dependence is reported for $D_{\text{Na,Ar}}$.

The helium (> 99.9%) and 90% Ne/10% He mixture (> 99.998%) are purified by a trap containing zeolite (50% 5X, 50% 13X molecular sieve) at 78 K. The nitrogen (> 99.999%) and argon (> 99.999%) are purified in the same trap at 193 K. The CO₂ (> 99.995%) is used without purification. The major impurities in the CO₂ are O₂, N₂, and H₂O, none of which have an exothermic second-order gas phase reaction with Na atoms. Na does react with O₂ in a thermomolecular reaction, but the rate is negligible at the low [O₂] and pressures in this study. For example, at 0.5 Torr total pressure, O₂ would have to be 1.4% of the carrier gas for the reaction to have a first-order rate constant of 5 s⁻¹. The effects of impurities are discussed further in Sec. V.

III. DATA ANALYSIS

The continuity equation for a species A in an axially symmetric cylindrical reactor under laminar flow conditions, suffering a first-order wall loss is¹¹

$$2v\left(1 - \frac{r^2}{a^2}\right) \frac{\partial A(r,z)}{\partial z} = \left[D \left(\frac{1}{r} \frac{\partial}{\partial r} r \frac{\partial}{\partial r} \right) + D \left(\frac{\partial^2}{\partial z^2} \right) \right] A(r,z), \quad (2)$$

where

z = axial coordinate,

r = radial coordinate, $r = 0$ at center of tube,

a = tube radius,

$A(r,z)$ = concentration of species A at (r,z) ,

D = diffusion coefficient of A in the carrier gas,

and

v = average flow velocity.

Equation (2) is subject to the boundary condition

$$D \frac{\partial A(r,z)}{\partial r} \bigg|_{r=a} = \frac{\gamma c A(r,z)}{2a(1 - \gamma/2)}, \quad (3)$$

where

γ = sticking probability for species A on the wall

and

c = mean molecular speed of A .

Equation (2) cannot be separated and solved in closed form. If the sticking coefficient γ is assumed to be unity, and axial diffusion is assumed to be a small effect, the approximate solution of Huggins and Cahn¹² can be used, and the diffusion coefficient is directly proportional to the observed wall loss rate

$$D = 0.272 a^2 k_{\text{obs}}. \quad (4)$$

Since γ appears in the boundary condition of the flow tube, the extraction of D from k_{obs} must be γ dependent. Indeed, the full numerical solution of Eq. (2) by Brown¹¹ has γ as a variable parameter. When $\gamma \approx 1$ the wall loss rate is diffusion controlled and the diffusion coefficient can be related to k_{obs} . Silver² has shown that D is insensitive to the exact value of γ when $0.1 < \gamma < 1.0$ and $D < 0.08 av$. A plot of D vs p^{-1} will only be linear for large D when $\gamma \approx 1$. In Sec. V we will use this to estimate γ .

For the measurement of $D_{\text{Na,Ne}}$ the carrier gas was a mixture of 90% Ne and 10% He. In the measurement of $D_{\text{Na,CO}_2}$ small amounts of He were present from the flush gas. The formula for the diffusion coefficient of a trace component in a multicomponent mixture is¹³

$$D_{A,\text{mixture}}^{-1} = \sum_i \frac{f_i}{D_{A,i}}, \quad (5)$$

where i is the gas index and f_i is the mole fraction of gas i . This formula was used to calculate $D_{\text{Na,Ne}}$ and $D_{\text{Na,CO}_2}$ from values measured in the Ne/He and CO₂/He mixtures. The reported values for $D_{\text{Na,Ne}}$ and $D_{\text{Na,CO}_2}$, therefore, depend on the measured value of $D_{\text{Na,He}}$, but the dependence is weak because the mole fraction of He was small. If $D_{\text{Na,He}}$ is changed by 10% the resulting change in $D_{\text{Na,Ne}}$ is less than 1%. $D_{\text{Na,CO}_2}$ is even less sensitive to $D_{\text{Na,He}}$ since f_{He} was always less than 0.05.

IV. RESULTS

At least 27 separate measurements of k_{obs} were made with each of the buffer gases, 90% Ne/10% He, N₂, and CO₂. Typical decay plots are shown in Fig. 1 and were quite linear. The flow tube pressure was varied between 0.14 and 6.3 Torr, and covered a range of at least a factor of 30 for each gas. Flow velocities ranged from 300 to 6000 cm s⁻¹. The diffusion coefficient was obtained from k_{obs} using Brown's program¹¹ and assuming $\gamma = 1$. This analysis al-

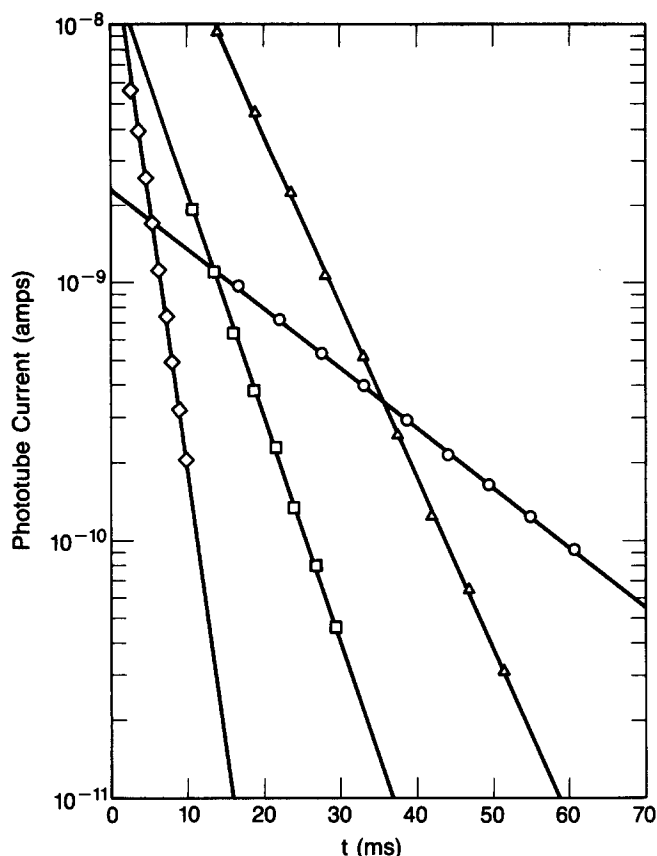


FIG. 1. Sample decay plots for different carrier gases and temperatures: (Δ) 90% Ne, 10% He, 0.771 Torr, 282 K, $v = 1070$ cm s $^{-1}$; (\circ) 96% CO $_2$, 4% He, 1.33 Torr, 281 K, 908 cm s $^{-1}$; (\square) He, 0.586 Torr, 211 K, $v = 1870$ cm s $^{-1}$; (\diamond) N $_2$, 0.153 Torr, 281 K, $v = 5600$ cm s $^{-1}$.

ways raises the diffusion coefficient relative to the solution of Huggins and Cahn,¹² Eq. (4). The diffusion coefficient calculated from Brown's program¹¹ is usually within 5% of the diffusion coefficient obtained from Eq. (4), although low pressure, high temperature measurements in He ($D \approx 3900$ cm 2 s $^{-1}$) had differences of up to 14%. D vs p^{-1} plots for Ne, N $_2$, and CO $_2$ are shown in Fig. 2. The reported diffusion coefficients, D_p (in units of cm 2 Torr s $^{-1}$), are the slopes of these plots. Tabulated results for $D_{Na,Ne}$, D_{Na,N_2} , and D_{Na,CO_2} are given in Table I.

For the measurement of $D_{Na,He}$ as a function of temperature, a total of 122 measurements of k_{obs} were performed at nine different temperatures. At least nine measurements of k_{obs} were made at each temperature. The measurements were made over a pressure range of 0.15–5.2 Torr and over a velocity range of 300–11 500 cm s $^{-1}$. The experimental results are summarized in Table II. D vs p^{-1} plots for He are shown in Fig. 3 for four different temperatures. Figure 4 is a plot of $\log D_p$ vs $\log T$ for $D_{Na,He}$. The observed temperature dependence of $D_{Na,He}$ is fit well by the expression $D_{Na,He}(T) = (385 \pm 40) (T/300)^{(1.72 \pm 0.18)}$ cm 2 Torr s $^{-1}$ as shown by the solid line in Fig. 4. The reported uncertainty in the temperature exponent is 2σ from the least squares fit. The uncertainty in $D(300$ K) reflects an estimate of random and systematic errors.¹

V. DISCUSSION

Measuring the diffusion coefficient over a large pressure range allows us to check for systematic errors in the experi-

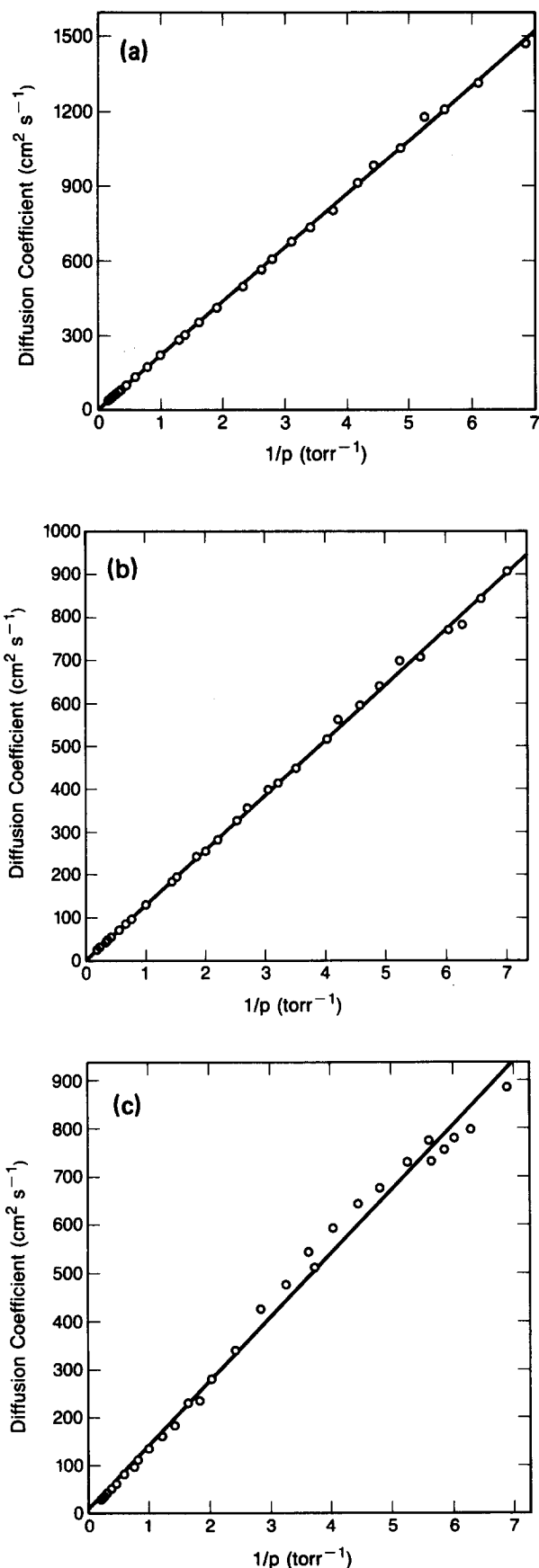


FIG. 2. D vs p^{-1} , D obtained from k_{obs} by method of Brown (see the text): (a) $D_{Na,Ne} = 209 \pm 21$ cm 2 Torr s $^{-1}$ at 281 K, $D_{Na,Ne}$ obtained from diffusion in 90% Ne, 10% He using Eq. (5); (b) $D_{Na,N_2} = 129 \pm 13$ cm 2 Torr s $^{-1}$ at 281 K; (c) $D_{Na,CO_2} = 134 \pm 13$ cm 2 Torr s $^{-1}$ at 281 K, D_{Na,CO_2} obtained from diffusion in > 95% CO $_2$, < 5% He using Eq. (5).

TABLE I. Na diffusion in Ne, N₂, and CO₂.

Carrier gas	<i>T</i> (K)	No. of expts.	<i>p</i> range (Torr)	D_p^a (cm ² Torr s ⁻¹)
Ne	282	27	0.15–6.3	209 ± 21
N ₂	281	30	0.14–5.3	129 ± 13
CO ₂	281	30	0.15–4.7	134 ± 13

^a Obtained from k_{obs} by the method of Brown as described in the text. Error limits represent 95% confidence level including an estimate for systematic errors.

ment and in the analysis. The intercepts of the D vs p^{-1} plots (Figs. 2 and 3) are not statistically different than zero at the 99% confidence level. This shows that the observed first-order Na loss is due only to diffusion controlled wall removal. A reactive impurity in the carrier gas leads to a functional dependence of the form $k_{\text{obs}} = aDp^{-1} + bp$, which yields a positive intercept in the limit of $p^{-1} \rightarrow 0$. Failure to observe such intercepts proves that the contribution from gas phase reaction with carrier gas impurities is completely negligible.

The low pressure experiments in CO₂ and the low pressure, high temperature experiments in He had pressure drops over the 35 cm measurement region of up to 4%. This does not introduce further uncertainties into the diffusion coefficient, since the experimental precision for the measurement of D is not dependent on the flow tube pressure.¹

Since the sticking coefficient γ is a variable parameter in Brown's program,¹¹ limits can be placed on its value by observing the effects it has on the transformation of k_{obs} into the diffusion coefficient. If we assume that the experimental data, when properly transformed to diffusion coefficients, would produce a linear D vs p^{-1} plot, one could, in principle,

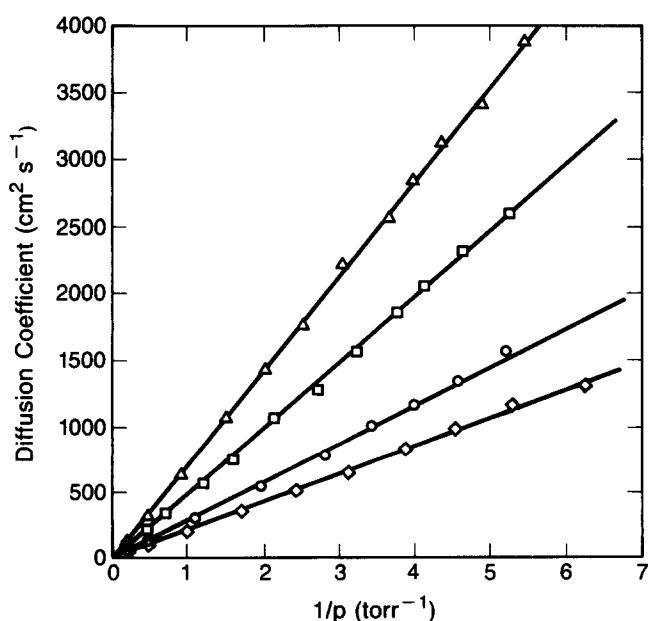


FIG. 3. D vs p^{-1} plots for Na diffusion in He at four temperatures, $D_{\text{Na,He}}$ obtained from k_{obs} by the method of Brown (see text): (Δ) $T = 424$ K, $D_{\text{Na,He}} = 712 \pm 71$ cm² Torr s⁻¹; (\square) $T = 332$ K, $D_{\text{Na,He}} = 499 \pm 50$ cm² Torr s⁻¹; (\circ) $T = 255$ K, $D_{\text{Na,He}} = 325 \pm 33$ cm² Torr s⁻¹; (\diamond) $T = 211$ K, $D_{\text{Na,He}} = 216 \pm 22$ cm² Torr s⁻¹.

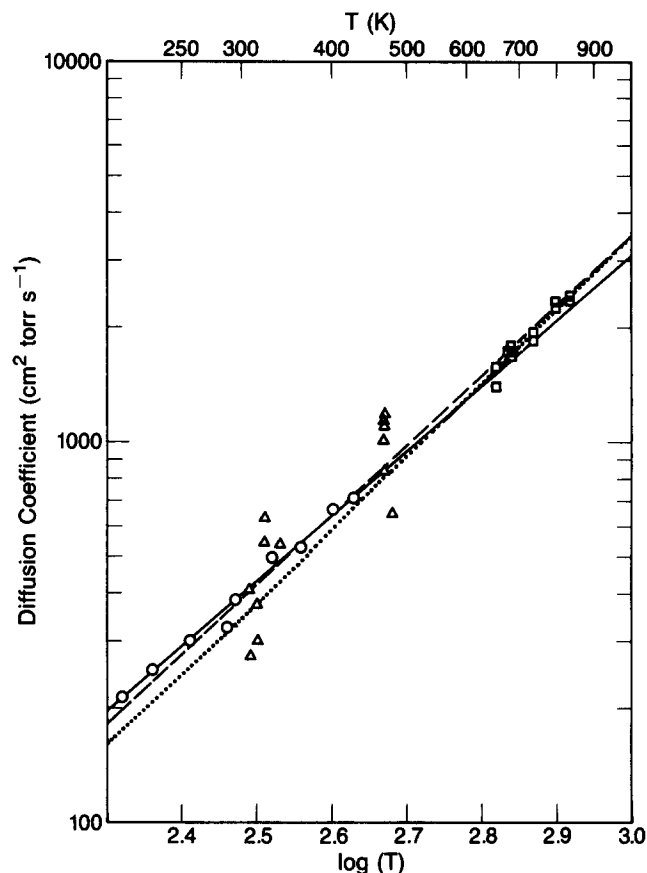


FIG. 4. Log $D_{\text{Na,He}}(T)$ vs log(T): (\circ) experimental results of this work, $T = 211$ –424 K; (Δ) results of Silver (Ref. 2), $T = 309$ –473 K; (\square) results of Kumuda *et al.* (Ref. 15), $T = 653$ –833 K; (—) best fit to data of this work; (.....) Chapman-Enskog calculations of this work using NaHe potential of Havey *et al.* (Ref. 25); (---) Chapman-Enskog calculations of Red'ko (Ref. 17).

solve for γ exactly. Large values of the diffusion coefficient measured at low pressures are most sensitive to changes in γ . For Ne and Ar, the γ 's that produced the best least squares fit to the D vs p^{-1} plot with the points weighted by D^{-1} were both 1.0. For Ne and CO₂ the optimal γ 's were 0.7 and 0.3. The effect of large changes in γ is illustrated in Fig. 5 for $D_{\text{Na,Ne}}$. Changing γ from 1 to 0.3 increases $D_{\text{Na,Ne}}$ obtained from a least squares fit of the D vs p^{-1} plot by 9%. When γ is

TABLE II. Summary of $D_{\text{Na,He}}$ as a function of temperature.

<i>T</i> (K)	No. of expts.	<i>p</i> range (Torr)	D_p^a (cm ² Torr s ⁻¹)
211	10	0.16–4.2	216 ± 22
229	10	0.15–5.2	255 ± 25
255	9	0.19–5.0	300 ± 30
290	36	0.19–4.8	325 ± 33
298	9	0.18–3.4	389 ± 39
332	12	0.19–5.0	499 ± 50
366	12	0.19–5.1	527 ± 53
396	12	0.22–5.2	663 ± 66
424	12	0.18–5.2	712 ± 71

^a Obtained from k_{obs} by the method of Brown (Ref. 11) as described in the text. Errors represent 95% confidence level including an estimate of systematic errors.

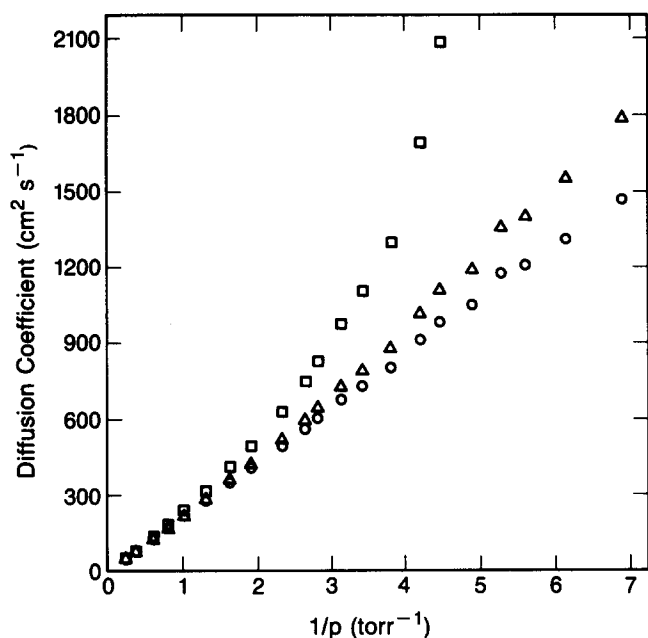


FIG. 5. Transformation of k_{obs} into $D_{\text{Na,Ne}}$ for different values of γ using the method of Brown (see text): (\square) $\gamma = 0.1$; (\triangle) $\gamma = 0.3$; (\circ) $\gamma = 1.0$.

changed to a value that changes D by more than 10%, the D vs p^{-1} graph becomes more curved at large values of D than can be reasonably accounted for by experimental errors and uncertainties. Since γ must be independent of the buffer gas, we conclude that γ is greater than 0.3 on the walls of our reactor and that it is probably close to 1. The linearity of the D vs p^{-1} plots for He in Fig. 3 shows that this conclusion is valid over the temperature range 211–426 K. The uncertainty in γ is taken into account in reporting the error limits on the D 's.

Table III is a comparison of our results for $D_{\text{Na,Ne}}$, $D_{\text{Na,N}_2}$, and $D_{\text{Na,CO}_2}$ with previous experimental work. Ex-

cept where noted, all the experimental values are extrapolated to 300 K for comparison using a $T^{1.7}$ temperature dependence, since it has been found for many gas phase systems¹⁴ that $D \propto T^{1.7}$. For $D_{\text{Na,N}_2}$ the agreement is excellent with the work of Silver,² who used a similar technique, and fairly good with the flash photolysis work of Husain *et al.*⁹ The agreement is only fair with the earlier work of Husain and Plane⁸ and with Hartel *et al.*³ Our value for $D_{\text{Na,Ne}}$ agrees with the results of most of the previous studies. The exceptions are the work of Husain *et al.*⁹ and Fairbank *et al.*⁶ The value reported by Husain *et al.*⁹ was based on a limited amount of data and extrapolated by the authors to 300 K using a $T^{1.5}$ temperature dependence. If a more realistic dependence of $T^{1.7}$ is employed, their value decreases to 120 $\text{cm}^2 \text{Torr s}^{-1}$ at 300 K, which makes the comparison poorer. Fairbank *et al.*⁶ report two values for $D_{\text{Na,Ne}}$ at 315 K, 323 and 428 $\text{cm}^2 \text{Torr s}^{-1}$, corresponding to experiments conducted on different days. It may be inferred from the large difference between these two numbers that their reported value has a considerable uncertainty. Our value of $D_{\text{Na,CO}_2}$ disagrees with the experimental study of Husain and Plane.⁸ As was discussed earlier¹ for $D_{\text{Na,He}}$, the values of $D_{\text{Na,CO}_2}$ published by Husain and Plane⁸ at 724 and 845 K imply a nonphysical temperature dependence of $T^{-7.3}$. Their reported values of $D_{\text{Na,CO}_2}$ can be assumed to have a large uncertainty.

The temperature dependence of $D_{\text{Na,He}}$ has been measured in two previous studies. Silver² obtained $D_{\text{Na,He}}(T) = (360 \pm 50)(T/300)^{1.75 \pm 0.02} \text{ cm}^2 \text{Torr s}^{-1}$ over the temperature range 309–473 K. Kumuda *et al.*,¹⁵ using the classic Stefan method, obtained $D_{\text{Na,He}}(T) = (385 \pm 40)(T/300)^{1.85 \pm 0.2} \text{ cm}^2 \text{Torr s}^{-1}$ over the temperature range 653–833 K. Both studies are in excellent agreement with our result of $D_{\text{Na,He}}(T) = (385 \pm 40)(T/300)^{1.72 \pm 0.18} \text{ cm}^2 \text{Torr s}^{-1}$ over the

TABLE III. Summary of experimentally measured diffusion coefficients for Na in Ne, N₂, and CO₂ normalized to 300 K.

Reference	Method ^a	T range (K)	p range (Torr)	$D_{\text{Na,Ne}}^b$ ($\text{cm}^2 \text{Torr s}^{-1}$)	$D_{\text{Na,N}_2}^b$ ($\text{cm}^2 \text{Torr s}^{-1}$)	$D_{\text{Na,CO}_2}^b$ ($\text{cm}^2 \text{Torr s}^{-1}$)
This work	Oven source, flow tube, RF	282	0.14–6.3	232 ± 23	144 ± 14	150 ± 15
Silver (Ref. 2)	Oven source, flow tube, LIF	320–698	1–8		165 ± 16	
Husain <i>et al.</i> (Ref. 9) ^c	Flash photolysis, resonant absorption	Ne:725,845 N ₂ :570–1016	8–400	144 ± 30	114 ± 38	
Husain and Plane (Ref. 8) ^c	Flash photolysis, resonant absorption	724,844	15–100		205,160	874,228
Cornellison (Ref. 7)	Static cell, laser absorption	530	3–30	292 ± 40		
Fairbank <i>et al.</i> (Ref. 6) ^d	Transit time of single atom across laser beam	315	100–400	346		
Bichi <i>et al.</i> (Ref. 5)	Spin relaxation	453	200	253		
Coolen and Hagedoorn (Ref. 10)	Nuclear reaction, LIF	300	110	266 ± 60		
Ramsey and Anderson (Ref. 4)	Spin relaxation	Ne:428 N ₂ :453	46–380	208	204	
Hartel <i>et al.</i> (Ref. 3)	Diffusion flame	655	1.4		183	

^a RF, resonant fluorescence; LIF, laser induced fluorescence.

^b Except when noted, extrapolated to 300 K using a temperature dependence of $T^{1.7}$; error limits are those of the authors, if reported.

^c Values are as reported for each temperature, extrapolations are those of the authors who used $T^{1.5}$.

^d Average of the two reported values.

temperature range 211–424 K. The results of Silver,² Kumada *et al.*,¹⁵ and the present work are shown in Fig. 4.

Chapman–Enskog theory relates the interatomic potential to the macroscopic transport properties: diffusion, thermal conductivity, and viscosity.¹⁶ To first order in the theory, the equation for the diffusion coefficient in units of cm² Torr s^{−1} for a two-parameter potential of the form $V(R) = \epsilon f(R/\sigma)$ is¹⁶

$$D_{1,2}(T) = \frac{1.997 [T^3(m_1 + m_2/2m_1m_2)]^{0.5}}{\sigma^2 \Omega_{12}^{(1,1)*}(T^*)}, \quad (6)$$

where m_1 and m_2 are the molecular weights of species 1 and 2 in amu, σ is in Å, T^* is the reduced temperature kT/ϵ , and $\Omega_{12}^{(1,1)*}(T^*)$ is a reduced collision integral. The higher order corrections to the calculated diffusion coefficients are less than 2% for Na–noble gas systems at near thermal energies.¹⁷ The reduced collision integral is a function of the interatomic potential and temperature, and its calculation, in general, is not simple. Fortunately, tabulated values of reduced collision integrals exist for many potentials including exponential,¹⁸ Morse,¹⁹ and $[m,6]$ and $[m,6,8]$ for $m = 9, 12, 15$, etc.^{20,21}

Ground state $^2\Sigma$ potentials for the NaHe, NaNe, and NaAr van der Waals molecules that can be used in Chapman–Enskog calculations have been extensively studied by theoretical and experimental methods. The well depth of the ground state is ~ 2 cm^{−1} in NaHe,²² 8.0 ± 0.3 cm^{−1} in NaNe,²³ and 39.8 cm^{−1} in NaAr.²⁴ The repulsive part of the potential dominates the scattering in Na + He and Na + Ne at thermal energies, while in Na + Ar scattering the larger attractive well is also important.

We have carried out Chapman–Enskog calculations using Na–noble gas potentials measured by quantitative spectroscopic methods and tabulated values of the collision integrals. For $D_{\text{Na,He}}$ and $D_{\text{Na,Ne}}$ the repulsive exponential potentials of Havey and co-workers^{25,26} obtained from line

broadening studies were used. Gottscho *et al.*²³ obtained a $[6,8]$ potential for NaNe from the molecular beam LIF data of Lapatovich *et al.*²⁷ We fit this potential to a $[6,9]$ form so the tables of Klein and Smith²⁰ could be used to calculate the reduced collision integral. We fit the NaAr line broadening data of York *et al.*²⁸ to a repulsive exponential to calculate $D_{\text{Na,Ar}}$. We also used the NaAr $X^2\Sigma$ Morse potential of Smalley *et al.*²⁹ which was obtained from molecular beam LIF data. The modified Morse potential of Tellinghuisen *et al.*,²⁴ which was obtained from a detailed analysis of the data of Smalley *et al.*,²⁹ could not be accurately fit to a $[m,6,8]$ form so the reduced collision integral was evaluated directly using the computer program of Rainwater *et al.*³⁰ Red'ko¹⁷ and Aret'ev and Guseva³¹ have done similar Chapman–Enskog calculations using the theoretical potentials of Refs. 32–34 and 35 and 36, respectively. The results of the Chapman–Enskog calculations of this work, of Red'ko,¹⁷ and of Aret'ev and Guseva³¹ are compared to our experimental values in Table IV.

The diffusion coefficients calculated from the NaHe and NaNe potentials of Havey and co-workers^{25,26} are in good agreement with our experimental results. $D_{\text{Na,Ne}}$ calculated from the potential of Gottscho *et al.*²³ is significantly lower than the measured value. This implies that the repulsive part of their potential rises too fast. As this LIF experiment is most sensitive to the shallow bound part of the $X^2\Sigma$ potential, one would not expect an accurate measurement of the repulsive wall which determines the scattering in Na + Ne. The NaAr potential of York *et al.*²⁸ predicts a value for $D_{\text{Na,Ar}}$ that is very close to the experimental value from our previous work.¹ The potential from the LIF experiment of Smalley *et al.*²⁹ predicts a value that is too low. However, the modified Morse potential of Tellinghuisen *et al.*²⁴ has a softer repulsive wall and the Chapman–Enskog calculation from this potential predicts $D_{\text{Na,Ar}} = 155$ cm² Torr s^{−1} which is in excellent agreement with the experimental value of 160 ± 16 cm² Torr s^{−1}, normalized to 300 K.

TABLE IV. Comparison of sodium–noble gas diffusion coefficients calculated using Chapman–Enskog theory with our experimental values. All values normalized to 300 K.

Gas	Reference	Interatomic potential Method ^a	Form	Calculated	D_p (cm ² Torr s ^{−1}) Measured	Reference
He	Havey <i>et al.</i> (Ref. 25) Krauss <i>et al.</i> (Ref. 33) Hanssen <i>et al.</i> (Ref. 34) Pascale and Vandeplanque (Ref. 32)	Line broadening Hartee–Fock Model potential Pseudopotential	Exponential Fit to standard forms ^{378b}	345	385 ± 40	This work Red'ko (Ref. 17)
Ne	Havey <i>et al.</i> (Ref. 26) Gottsho <i>et al.</i> (Ref. 23) Pascale and Vandeplanque (Ref. 32)	Line broadening Molecular beam, LIF Pseudopotential	Exponential [6,8] Fit to standard form	217 189 236	232 ± 23	This work This work Red'ko (Ref. 17)
Ar	York <i>et al.</i> (Ref. 28) Smalley <i>et al.</i> (Ref. 29) Tellinghuisen <i>et al.</i> (Ref. 24) Pascale and Vandeplanque (Ref. 32) Saxon <i>et al.</i> (Ref. 35) Laskowski <i>et al.</i> (Ref. 36)	Line broadening Molecular beam, LIF Analysis of data of Smalley <i>et al.</i> Pseudopotential SCF/CI SCF/CI	Exponential Morse Modified Morse Fit to standard form Fit to standard form Fit to standard form	151 131 155 135 166 145	160 ± 16	This work This work This work Red'ko (Ref. 17) Aret'ev and Guseva (Ref. 31) Aret'ev and Guseva (Ref. 31)

^a LIF, laser induced fluorescence; SCF/CI, self-consistent field with configuration interaction.

^b Author apparently averaged values from the three theoretical potentials.

Red'ko¹⁷ used the Hartree-Fock potential of Krauss *et al.*³³ and the semiempirical potentials of Hanssen *et al.*³⁴ and Pascale and Vandeplanque³² to calculate $D_{\text{Na,He}}$. The potentials of Pascale and Vandeplanque³² were used to calculate $D_{\text{Na,Ne}}$ and $D_{\text{Na,Ar}}$. The calculated values of $D_{\text{Na,He}}$ and $D_{\text{Na,Ne}}$ are in excellent agreement with our experimental results. This good agreement shows that although the potential calculations were not sophisticated, they provide an accurate description of the low energy (up to $\sim 1000 \text{ cm}^{-1}$) part of the repulsive wall that determines the scattering at thermal energies. However, the NaAr potential of Pascale and Vandeplanque³² is not adequate to describe thermal Na-Ar scattering; Red'ko's¹⁷ calculations using this potential predict a value of $D_{\text{Na,Ar}}$ that is too low. Aret'ev and Guseva³¹ used the more sophisticated SCF/CI potentials of Saxon *et al.*³⁵ and Laskowski *et al.*³⁶ to calculate $D_{\text{Na,Ar}}$. The potential of Saxon *et al.*³⁵ predicts a value of $D_{\text{Na,Ar}}$ that is in excellent agreement with the experimental result. The potential of Laskowski *et al.*,³⁶ which did not reproduce the experimentally observed potential minimum of 40 cm^{-1} , predicts a value of $D_{\text{Na,Ar}}$ that is too low.

It is a more rigorous test of the NaHe potentials to predict the temperature dependence of $D_{\text{Na,He}}$. Chapman-Enskog calculations using the potential of Havey *et al.*²⁵ predict a temperature exponent of 1.88 while the calculations of Red'ko¹⁷ predict a temperature exponent of 1.82. Both values are higher than the 1.72 ± 0.18 observed in this work and the 1.75 ± 0.02 observed by Silver,² although they are within the uncertainty limits of this work. The results of both calculations are compared to the experimental results of Kumuda *et al.*,¹⁵ Silver,² and the present study in Fig. 4. The small differences among the predicted and experimentally measured temperature exponents are not considered significant, since the results of both calculations provide a reasonable fit to the experimental data. Still, the calculations of Red'ko¹⁷ are in the best agreement with the experimental data. This shows that the simple theoretical potentials of Refs. 32–34 accurately describe the low energy part of the repulsive wall that determines the scattering in Na + He.

We are surprised that $D_{\text{Na,CO}_2}$ is as large as $D_{\text{Na,N}_2}$. The hard sphere radii of CO₂ and N₂ can be estimated from their diffusion coefficients in He and H₂.^{14,37} This calculation yields $r_{\text{CO}_2} \approx 2.0 \text{ \AA}$ and $r_{\text{N}_2} \approx 1.7 \text{ \AA}$. However, using Eq. (6) with our experimental data implies that the collision cross section Na + N₂ is 14% larger than the collision cross section for Na + CO₂. The larger Na collision cross section for N₂, the smaller molecule, is difficult to explain in the absence of any work on the NaN₂ and NaCO₂ potentials.

ACKNOWLEDGMENTS

We thank Dr. James C. Rainwater for his assistance in performing the Chapman-Enskog calculations. This work

was supported in part by the Chemical Manufacturers Association Panel on Fluorocarbon Research.

- ¹C. L. Talcott, J. W. Ager III, and C. J. Howard, *J. Chem. Phys.* **84**, 6161 (1986).
- ²J. A. Silver, *J. Chem. Phys.* **81**, 5125 (1984).
- ³H. Hartel, N. Meer, and M. Polanyi, *Z. Phys. Chem. (Leipzig)* **199**, 139 (1932).
- ⁴A. T. Ramsey and L. W. Anderson, *Nuovo Cimento* **32**, 1151 (1964).
- ⁵P. Bichi, L. Moi, P. Savino, and B. Zambon, *Nuovo Cimento B* **55**, 1 (1980).
- ⁶W. M. Fairbank, C. Y. She, and J. V. Prodan, *Proc. SPIE Int. Soc. Opt. Eng.* **286**, 94 (1981).
- ⁷H. J. Cornelissen, *16th International Conference on Ionization Phenomenon*, edited by W. Boettcher, H. Wenk, and E. Guide (University of Dusseldorf, Dusseldorf, 1983), p. 52; *Bull. Am. Phys. Soc.* **30**, 128 (1985).
- ⁸D. Husain and J. M. C. Plane, *J. Chem. Soc. Faraday Trans. 2* **78**, 163 (1982).
- ⁹D. Husain, P. Marshall, and J. M. C. Plane, *J. Chem. Soc. Faraday Trans. 2* **81**, 301 (1985).
- ¹⁰F. C. M. Coolen and H. L. Hagedoorn, *Physica C (Utrecht)* **79**, 402 (1975).
- ¹¹R. L. Brown, *J. Res. Natl. Bur. Stand.* **83**, 1 (1978).
- ¹²R. W. Huggins and J. H. Cahn, *J. Appl. Phys.* **38**, 180 (1967).
- ¹³D. F. Fairbank and C. R. Wilke, *Ind. Eng. Chem.* **42**, 471 (1950).
- ¹⁴T. R. Marrero and E. A. Mason, *J. Phys. Chem. Ref. Data* **1**, 3 (1972).
- ¹⁵T. Kumuda, R. Ishiguro, and Y. Kimachi, *Nucl. Sci. Eng.* **70**, 73 (1979).
- ¹⁶J. O. Hirschfelder, C. F. Curtiss, and R. B. Bird, *Molecular Theory of Gases and Liquids* (Wiley, New York, 1954), p. 539.
- ¹⁷T. P. Red'ko, *Opt. Spectrosc.* **52**, 769 (1982) [*Opt. Spectrosc. (USSR)* **52**, 461 (1982)]; *Zh. Tekh. Fiz.* **53**, 1730 (1983) [*Sov. Phys. Tech. Phys.* **28**, 1065 (1983)].
- ¹⁸L. Monchick, *Phys. Fluids* **2**, 695 (1959).
- ¹⁹F. J. Smith and R. J. Munn, *J. Chem. Phys.* **41**, 3560 (1964).
- ²⁰M. Klein and F. J. Smith, *J. Res. Natl. Bur. Stand. Sect. A* **72**, 359 (1968).
- ²¹M. Klein, H. J. M. Hanley, F. J. Smith, and P. Holland, *Natl. Bur. Stand. (U.S.) (U.S. GPO Washington, D.C., 1974)*, Vol. 47, pp. 1–157.
- ²²J. Pascale, *Phys. Rev. A* **28**, 632 (1983).
- ²³R. A. Gottscho, R. Ahmad-Bitar, W. P. Lapatovich, I. Renhorn, and D. E. Pritchard, *J. Chem. Phys.* **75**, 2546 (1981).
- ²⁴J. Tellinghuisen, A. Ragone, M. S. Kim, D. J. Auerbach, R. E. Smalley, L. Wharton, and D. H. Levy, *J. Chem. Phys.* **71**, 1283 (1979).
- ²⁵M. D. Havey, S. E. Frolking, and J. J. Wright, *Phys. Rev. Lett.* **45**, 1783 (1980).
- ²⁶M. D. Havey, S. E. Frolking, J. J. Wright, and L. C. Balling, *Phys. Rev. A* **24**, 3105 (1981).
- ²⁷W. P. Lapatovich, R. Ahmad-Bitar, P. E. Moskovich, I. Renhorn, R. A. Gottscho, and D. E. Pritchard, *J. Chem. Phys.* **73**, 5419 (1980).
- ²⁸G. York, R. Scheps, and A. Gallagher, *J. Chem. Phys.* **63**, 1052 (1975).
- ²⁹R. E. Smalley, D. A. Auerbach, P. S. H. Fitch, D. H. Levy, and L. Wharton, *J. Chem. Phys.* **66**, 3778 (1977).
- ³⁰J. C. Rainwater, P. M. Holland, and L. Biolsi, *J. Chem. Phys.* **77**, 434 (1980).
- ³¹K. M. Aret'ev and M. A. Guseva, *Inzh. Fiz. Zh.* **47**, 608 (1984).
- ³²J. Pascale and J. Vandeplanque, *J. Chem. Phys.* **60**, 2278 (1974).
- ³³M. Krauss, P. Maldonado, and A. C. Wahl, *J. Chem. Phys.* **54**, 4944 (1971).
- ³⁴J. Hanssen, R. McCarroll, and P. Valiron, *J. Phys. B* **12**, 899 (1971).
- ³⁵R. P. Saxon, R. E. Olson, and B. Lie, *J. Chem. Phys.* **67**, 2692 (1977).
- ³⁶B. C. Laskowski, S. R. Langhoff, and J. R. Stallcop, *J. Chem. Phys.* **75**, 815 (1981).
- ³⁷E. W. McDaniel, *Collision Phenomena in Ionized Gases* (Wiley, New York, 1964), p. 50.